Constitutive Dimerization of the G-Protein Coupled Receptor, Neurotensin Receptor 1, Reconstituted into Phospholipid Bilayers

Peter J. Harding,[†] Helen Attrill,[†] Jonas Boehringer,[†] Simon Ross,[†] George H. Wadhams,[‡] Eleanor Smith,[†] Judith P. Armitage,[‡] and Anthony Watts[†*]
[†]Biomembrane Structure Unit, and [‡]Microbiology Unit, Department of Biochemistry, University of Oxford, Oxford, United Kingdom

ABSTRACT Neurotensin receptor 1 (NTS1), a Family A G-protein coupled receptor (GPCR), was expressed in *Escherichia coli* as a fusion with the fluorescent proteins eCFP or eYFP. A fluorophore-tagged receptor was used to study the multimerization of NTS1 in detergent solution and in brain polar lipid bilayers, using fluorescence resonance energy transfer (FRET). A detergent-solubilized receptor was unable to form FRET-competent complexes at concentrations of up to 200 nM, suggesting that the receptor is monomeric in this environment. When reconstituted into a model membrane system at low receptor density, the observed FRET was independent of agonist binding, suggesting constitutive multimer formation. In competition studies, decreased FRET in the presence of untagged NTS1 excludes the possibility of fluorescent protein-induced interactions. A simulation of the experimental data indicates that NTS1 exists predominantly as a homodimer, rather than as higher-order multimers. These observations suggest that, in common with several other Family A GPCRs, NTS1 forms a constitutive dimer in lipid bilayers, stabilized through receptor-receptor interactions in the absence of other cellular signaling components. Therefore, this work demonstrates that well-characterized model membrane systems are useful tools for the study of GPCR multimerization, allowing fine control over system composition and complexity, provided that rigorous control experiments are performed.

INTRODUCTION

G-protein coupled receptors (GPCRs), of which more than 750 have been identified in the human genome (1), are a family of integral membrane proteins with seven transmembrane helices. GPCRs are involved in a wide range of physiological processes, including cell-cell communication, sensory transduction, neuronal transmission, and hormonal signaling (2,3), and are consequently of particular pharmacological importance (4).

Neurotensin (NT) is an endogenous tridecapeptide neurotransmitter (N-Glu-Leu-Tyr-Glu-Asn-Lys-Pro-Arg-Arg-Pro-Tyr-Ile-Leu-C), found in mammalian gastrointestinal, cardiovascular, and central nervous systems, that is responsible for the activation of the neurotensin receptor (NTS) family (5). One such receptor, neurotensin receptor type 1 (NTS1), binds NT with high affinity (K_d = 1 nM), and is a member of the GPCR superfamily (6).

The suggestion that GPCRs function as isolated monomeric receptors in the cell membrane has been challenged by results consistent with GPCRs functioning as dimers or higher-order oligomers, and the subject was recently reviewed in detail (7–10). GPCR multimerization is thought to have important functional implications, including cell-surface expression, ligand binding, signaling, and receptor trafficking (8). Although the concept of multimerization is widely accepted, considerable variation exists between reports of the effects of agonist ligands on the multimerization state. There are some examples of agonist-mediated multimerization, e.g., as described for purified leukotriene B_4 receptor (11), and agonist-mediated monomerization, as described in an initial study of the δ-opioid receptor (12). However, constitutive multimerization has been most widely reported.

GPCR multimerization was demonstrated for numerous receptor types using biochemical approaches, including co-immunoprecipitation (13) and functional complementation (14,15). Resonance energy transfer (RET) techniques, such as fluorescence resonance energy transfer (FRET) and bioluminescence resonance energy transfer (BRET), were used to probe GPCR multimerization in vivo (16,17). However, some criticism of the methodologies used to demonstrate multimerization has been made, including the possibility of nonspecific aggregation, incomplete solubilization, or insufficient centrifugation during immunoprecipitation procedures (9). In addition, a study involving the rigorous treatment of BRET data suggested that the multimerization of GPCRs may not be as prevalent as previously reported using RET techniques, because of the underestimation of energy transfer caused by random interactions of receptors in the membrane environment (16). This serves to highlight that the extent of GPCR multimerization is by no means fully understood. There are, to the best of our knowledge, no published data regarding NTS1 homomultimerization in the lipid membrane environment. Immunoprecipitation studies suggested possible heterodimerization with other members of the NTS family (18,19), and one study indirectly revealed NTS1 monomers and dimers in detergent solution under certain conditions (20).

The majority of GPCR multimerization studies to date have been performed in transfected cell lines (10). The study of GPCR multimerization, using well-characterized in vitro

Submitted June 17, 2008, and accepted for publication September 22, 2008.

*Correspondence: anthony.watts@bioch.ox.ac.uk

Editor: David D. Thomas.

0006-3495/09/02/0964/10 $2.00

doi: 10.1016/j.bpj.2008.09.054

systems, potentially allows for the rigorous study of the mechanism of multimerization, while maintaining fine control of system conditions and components. Such fine control over system parameters, including receptor density, lipid composition, and donor/acceptor ratio, is of particular advantage, given the multitude of controls considered necessary to confirm that an observed RET arises from true receptor-receptor interactions (16). Indeed, a recent FRET study of rhodopsin photoreceptors reconstituted into asolectin liposomes revealed receptor self-association (21).

Here, purified NTS1 receptor, tagged with enhanced cyan fluorescent protein (eCFP) and enhanced yellow fluorescent protein (eYFP), is used to develop an in vitro system for the study of the NTS1 multimerization state in lipid bilayers. This FRET study of eCFP-tagged and eYFP-tagged NTS1, reconstituted into brain polar lipid liposomes at low receptor density, provides evidence that NTS1 receptors constitutively self-associate in the membrane environment in an agonist-independent manner.

MATERIALS AND METHODS

Reconstitution of T43NTS1, T43NTS1-eCFP, and T43NTS1-eYFP

The N-terminally truncated NTS1 (T43NTS1) (22–24), T43NTS1-eCFP, and T43NTS1-eYFP (24) (Fig. 1 *A*) were expressed, detergent-solubilized, and purified as described (see the Supporting Material). Purified T43NTS1, T43NTS1-eCFP, and T43NTS1-eYFP receptors, mixed to the desired ratios, were added to disrupted brain polar lipid (BPL) vesicles (prepared as described in the Supporting Material), and samples were incubated for 1 h at 4°C. Prewashed Biobeads (SM-2, Biorad, Hemel Hempstead, UK) were added to a concentration of 120 mg/mL, and samples were incubated at 4°C overnight with gentle agitation. The Biobeads were removed, and the proteoliposomes were isolated by sucrose density gradient centrifugation (5–35% sucrose in 50 mM Tris, pH 7.4, 200 mM NaCl, and 1 mM EDTA; 100,000 × *g*; 4°C; 15 h). Receptor density was derived by measurement of the position of reconstituted bands on the sucrose gradient (see the Supporting Material).

Fluorescence measurements

All FRET experiments were performed using an LS-55 Spectrofluorimeter (Perkin Elmer, Fremont, CA) and a 1.5-mL quartz microcuvette (Hellma, Southend-on-Sea, UK) with a magnetic stir bar. The cuvette was maintained at a constant temperature throughout, using a recirculating water-chiller set at 4°C. Excitation and emission slits were both set to a 2.5-nm bandpass. Before the fluorescence measurements, receptor samples were diluted to the stated receptor concentrations, using 50 mM Tris (pH 7.4), 15% glycerol (v/v), 200 mM NaCl, 0.1% dodecyl-β-D-maltoside (DDM) (w/v), 0.01% cholesteryl hemisuccinate (CHS) (w/v), and 1 mM EDTA for detergent samples, and 50 mM Tris (pH 7.4), 200 mM NaCl, and 1 mM EDTA for reconstituted samples. To assess the effect of neurotensin peptide (NT) on multimerization, an appropriate volume of NT stock solution (3.5 mM) was added, and samples were allowed to equilibrate for 15 min before measurement. All fluorescence spectra were recorded in triplicate and averaged.

The FRET protocol was a variation of that proposed previously (17), where FRET is quantified by monitoring enhanced acceptor emission (''sensitized emission''). In each FRET experiment, fluorescence emission spectra are recorded from four separate samples: 1), a buffer-only blank; 2), a sample containing only NTS1-eCFP; 3), a sample containing only NTS1-eYFP; and 4), a sample containing both NTS1-eCFP and NTS1-eYFP. Fluorescence emission, because of FRET between eCFP-tagged and eYFP-tagged receptors, was detected by using a procedure to remove contributions of background signal, eCFP emission (''bleed-through''), and direct eYFP emission (''cross talk'') from the eCFP-tagged and eYFP-tagged sample emission spectrum. This was achieved as follows:

1. Subtraction of background fluorescence: Emission spectra for all samples were recorded between 450–600 nm, using an excitation wavelength of

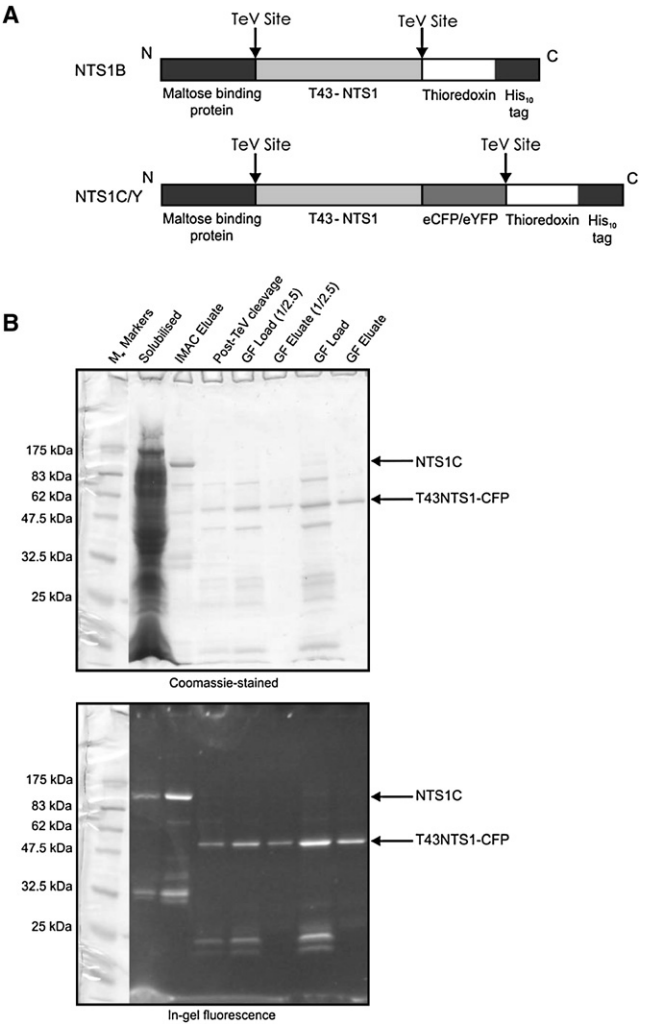

FIGURE 1 Analysis of an example of purification of T43NTS1-eCFP. (*A*) Schematic depiction of untagged NTS1B construct (22) and fluorescence-tagged NTS1C and NTS1Y constructs. Genes for eCFP and eYFP were introduced into the NTS1B construct, to yield NTS1C and NTS1Y constructs. The TeV protease cleavage sites present between the *E. coli* maltose-binding protein (MBP) and T43NTS1 moieties and the eCFP/eYFP and *E. coli* thioredoxin (TrxA) moieties facilitate proteolytic removal of the fusion partners (T43NTS1, N-terminally truncated NTS1; His_{10}, deca-histidine tag). (*B*) SDS-PAGE analysis of purification, showing how overexpression and purification were monitored using in-gel fluorescence. Indicated fractions from T43NTS1-eCFP purification of an *E. coli* C41(DE3) culture were separated on a 12% SDS-PAGE gel. In-gel fluorescence (*bottom*) was monitored, and the gel was subsequently stained with Coomassie brilliant blue (*top*). The NTS1C protein is evident in the solubilized and immobilized metal affinity chromatography (IMAC) elution samples (theoretical molecular mass, 130 kDa). In post-TeV cleavage, GF load, and gel filtration (GF) eluate lanes, the T43NTS1-eCFP cleavage product (theoretical molecular mass, 69.9 kDa) is evident (31,32).

440 nm (λ_{max}^{CFP}), and between 520–600 nm, using an excitation wavelength of 510 nm (λ_{max}^{YFP}). The background emission obtained from sample 1 was then subtracted from samples 2–4 for both emission spectra.

2. Subtraction of ''bleed-through'': The emission spectrum obtained from the excitation of sample 2 at λ_{max}^{CFP} was normalized to give an eCFP emission peak value identical to the eCFP emission peak value of sample 4. After normalization, the eCFP spectrum of sample 2 was subtracted from the emission spectrum of sample 4. This resulted in an eYFP emission spectrum composed of a FRET component and a ''cross talk'' component because of direct excitation of eYFP, which can also be termed the ''extracted acceptor spectrum''.
3. Subtraction of ''cross talk'': The emission spectra yielded from the excitation of samples 3 and 4 at λ_{max}^{YFP} were used to quantify the amount of eYFP-tagged receptor present in each sample. This is possible because eCFP is not excited at this wavelength. The ratio of the eYFP emission peak heights of these two spectra were used as a scaling factor to normalize the emission spectrum obtained when sample 3 was irradiated at λ_{max}^{CFP}. This normalized spectrum, which corresponds to the ''cross talk'', was then subtracted from the extracted acceptor spectrum obtained in the previous section. This results in an eYFP emission spectrum attributable solely to FRET.

Measurement of donor/acceptor ratio

The donor/acceptor ratios of the T43NTS1-eCFP/eYFP detergent samples were calculated by comparing the fluorescence intensity of the maximal eCFP and eYFP emissions (when excited at λ_{max}^{CFP} and λ_{max}^{YFP}, respectively). The fluorescence intensities (F) of eCFP and eYFP were corrected using the fluorophore quantum yields (Φ) and the fluorophore molar extinction coefficients at λ_{max}^{CFP} and λ_{max}^{YFP} (ε), using Eq. 1 (eCFP, $\Phi = 0.4$, $\varepsilon =$ 29,817 $M^{-1}cm^{-1}$ (25–27); eYFP $\Phi = 0.61$, $\varepsilon = 75{,}768$ $M^{-1}cm^{-1}$ (27,28)):

$$F = c\Phi_D\varepsilon. \quad (1)$$

The donor/acceptor ratios of reconstituted samples were calculated in a similar manner. However, the calculated donor fluorescence intensity was corrected using the known FRET signal observed for each sample, to take into account the decrease in donor emission because of FRET. This involved summation of the observed eCFP fluorescence with the FRET emission curve, after correction of the FRET signal to allow for the difference in extinction coefficient between donor and acceptor, thereby yielding the eCFP fluorescence intensity in the absence of FRET. This could then be related directly with the maximal eYFP emission, using Eq. 1.

Calculation of FRET efficiency

To allow direct comparison between experiments and with other multimerization studies of GPCRs in vivo, a parameter termed the ''apparent FRET efficiency'' was calculated (17). This does not measure the precise efficiency of FRET, and is therefore not useful for interfluorophore distance measurements. However, it is a rapid method for the comparison of the relative ability of GPCRs to engage in FRET. Apparent FRET efficiency was calculated as follows:

$$E^{app} = \frac{F_{DA}^{FRET}}{F_{DA}^{A}} \times 100, \quad (2)$$

where E^{app} is the apparent FRET efficiency, F_{DA}^{FRET} is the fluorescence intensity attributable to FRET, and F_{DA}^{A} is the fluorescence intensity of the acceptor when excited at λ_{max}^{YFP}.

The corrected FRET efficiency was calculated as follows (29,30):

$$E = \left(\frac{\varepsilon_A}{\varepsilon_D}\right)\left(\frac{F_{DA}^{FRET}}{F_{DA}^{A}}\right), \quad (3)$$

where E is the corrected FRET efficiency, ε_A is the molar extinction coefficient of eYFP at λ_{max}^{YFP} (75,768 $M^{-1}cm^{-1}$ (27)), and ε_D is the molar extinction coefficient of the donor at λ_{max}^{CFP} (29,817 $M^{-1}cm^{-1}$ (25)). The corrected FRET efficiency was used to calculate the average interfluorophore distance:

$$R = R_o\left(\frac{1}{E} - 1\right)^{\frac{1}{6}}, \quad (4)$$

where R is the average distance between donor and acceptor, and R_o is the Förster distance for the eCFP/eYFP FRET pair, which was calculated as described in the Supporting Material.

Radioligand binding assays

A ^{3}H-NT (New England Nuclear, Perkin Elmer, Waltham, MA) radioligand binding assay was used to quantify amounts of active receptor present throughout the purifications. Samples were incubated in assay buffer (50 mM Tris, pH 7.4, 0.1% DDM (w/v), 0.01% CHS (w/v), 1 mM EDTA, and 0.1 mg/mL bovine serum albumin) containing ^{3}H-NT to a final concentration of 5 nM (1 h, 4°C). Detergent was omitted from the buffer for reconstituted samples. Nonspecific binding was quantified in the presence of excess unlabeled NT (3.5 μM). Separation of bound from free ligand was achieved by gel filtration, using P30 Tris spin columns (BioRad) for detergent-solubilized fractions, and by filtration, using Durapore PVDF membranes with a 0.2-μm molecular mass cutoff (Millipore, Carrigtwohill, Ireland) for reconstituted samples.

In-gel fluorescence

The fluorescence of eCFP and eYFP moieties was monitored by in-gel fluorescence (31,32), using standard Tris-Glycine SDS PAGE (Invitrogen, Paisley, UK). The eCFP-His_6/eYFP-His_6 standards were loaded onto the same gel, to allow quantification of the amount of fluorescent protein present in receptor samples. To detect fluorescent bands, the gel was illuminated with ultraviolet light, and images were captured with a CCD camera system (Gel Doc, BioRad). Fluorescence intensities were quantified using ImageJ software version 1.36b (National Institutes of Health, Bethesda, MD), and the gels were subsequently stained with Coomassie brilliant blue.

RESULTS

Production of NTS1 labeled with fluorescent proteins

The T43NTS1-eCFP and T43NTS1-eYFP (24) were expressed in *Escherichia coli* as the fusion proteins NTS1C and NTS1Y (Fig. 1 *A*). After detergent solubilization and purification by nickel-affinity chromatography, the fusion proteins were removed, using tobacco etch virus (TeV) protease cleavage, and the resulting T43NTS1-eCFP and T43NTS1-eYFP proteins were isolated from the cleavage products, using gel-filtration chromatography. Purification was monitored using a radioligand binding assay and in-gel fluorescence (Fig. 1 *B*) (32). A typical purification from 20 g of cell pellet yielded 8.6 ± 0.5 nmol (0.6 ± 0.04 mg) of cleaved, fluorescence-tagged receptor, as determined by in-gel fluorescence.

Radioligand binding analysis confirmed the high affinity of purified fluorescent receptor for NT, both before (K_d = 0.5 ± 0.2 nM) and after (K_d = 0.6 ± 0.2 nM) reconstitution (Fig. 2 *A*). These affinities compared well with the affinity of

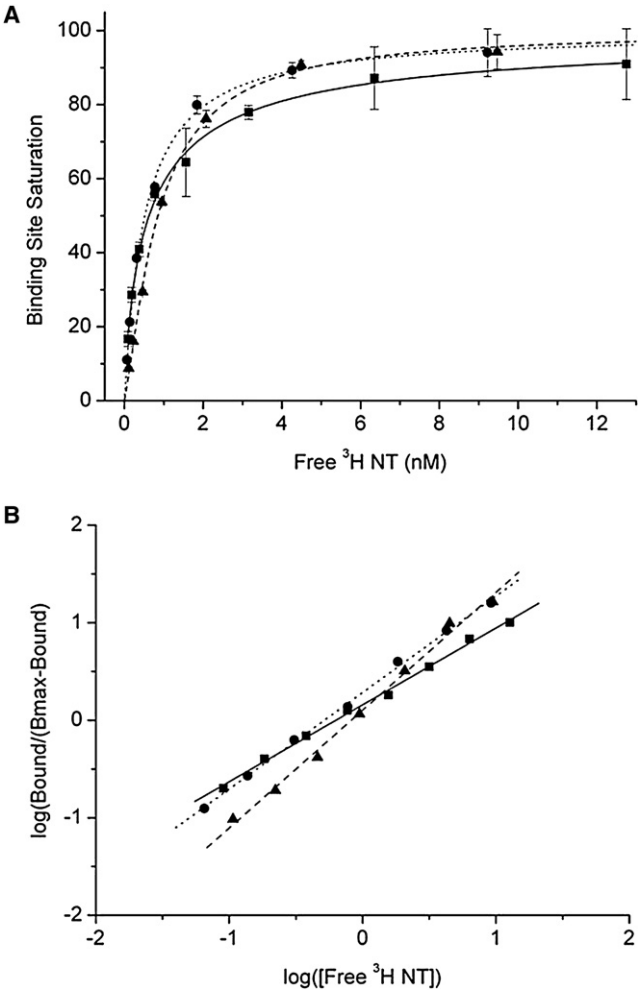

FIGURE 2 Radioligand ligand-binding data for detergent-solubilized and reconstituted NTS1: ■ and solid line, reconstituted NTS1-eYFP; ● and dotted line, detergent-solubilized NTS1-eYFP; ▲ and dashed line, detergent-solubilized NTS1. (*A*) Saturation binding of tritiated NT to receptor samples. Data were fitted to Langmuir isotherms to give a measure of binding affinity. (*B*) Hill plot for binding data.

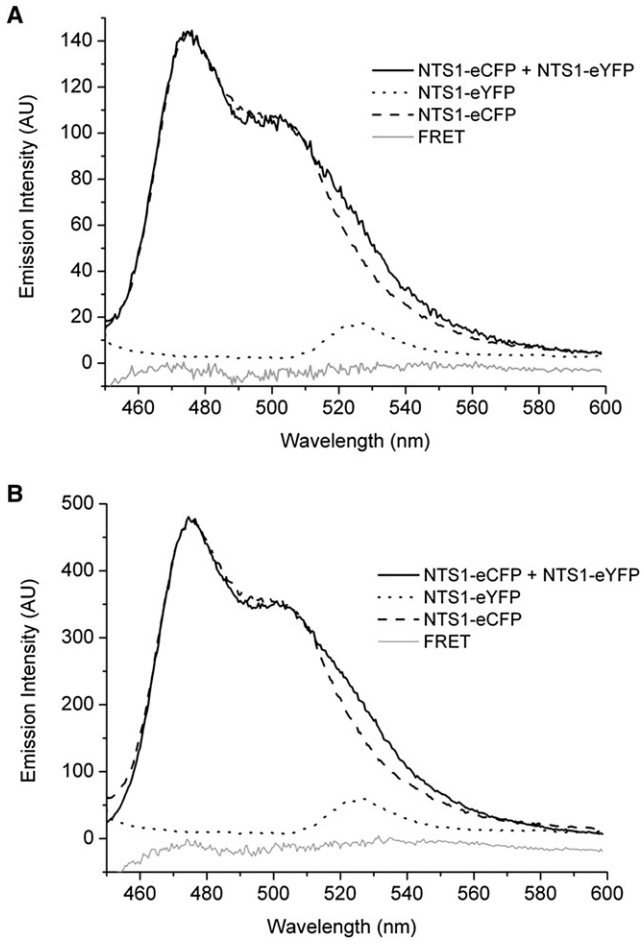

FIGURE 3 Use of FRET to detect multimerization of purified T43NTS1-eCFP and T43NTS1-eYFP in detergent solution at concentrations of 60 nM (*A*) and 200 nM (*B*). Samples were excited at λ_{max}^{CFP} (440 nm), and fluorescence emission was detected by scanning fluorometry. Fluorescence emission attributable to FRET (*gray solid line*) was determined by subtracting normalized emission spectrum of a T43NTS1-eCFP sample (*black dashed line*) and normalized emission spectrum of a T43NTS1-eYFP sample (*black dotted line*) from the emission spectrum of the mixed T43NTS1-eCFP and T43NTS1-eYFP sample (*black solid line*).

nonfluorescent NTS1 for NT (1.0 ± 0.2 nM) (Fig. 2 *A*), as well as the affinities for the NT-NTS1 interaction reported previously (6,33–35). Saturation binding experiments for all samples gave Hill numbers of ~1 (Fig. 2 *B*), with reconstituted NTS1-eYFP, detergent-solubilized NTS1-eYFP, and detergent-solubilized NTS1 yielding Hill numbers of 1.2 ± 0.1, 0.8 ± 0.1, and 1.0 ± 0.1, respectively, indicating that one receptor binds one ligand molecule with no cooperativity.

NTS1 is monomeric in detergent solution

The FRET experiments were performed on purified, fluorescence-tagged receptors in detergent solution. Fig. 3 shows the emission spectra for the mixed T43NTS1-eCFP and T43NTS1-eYFP sample (eCFP/eYFP molar ratio of 1:1 ± 0.02) excited at 440 nm, and the corresponding subtractions of ''bleed through'' and ''cross talk'' to yield the eYFP emission attributable to FRET. It is evident from the baseline emission spectrum after subtraction (Fig. 3) that, at a concentration of 60 nM and a higher concentration of 200 nM, no FRET occurred. Repetition of the experiment in the presence of 10 μM agonist (NT) also failed to show any FRET between eCFP-tagged and eYFP-tagged receptors. These results together indicate that the interfluorophore distance between the eCFP and eYFP tags is too large for FRET to occur (>100 Å), and therefore the receptor is monomeric in detergent solution over this concentration range, with no sample aggregation. In addition, agonist binding does not trigger multimerization of the detergent-solubilized receptor, at least within the timescale of the FRET experiment (up to 1 h, 4°C).

NTS1 forms a constitutive multimer in BPL proteoliposomes

Purified fluorescent receptor was reconstituted into BPL liposomes, using a strategy based on partial vesicle solubilization (36,37). Detergent was removed by hydrophobic adsorption, using polystyrene beads (38) and proteoliposomes isolated using sucrose density gradient centrifugation (Fig. 4 *A*). Analysis of the resulting proteoliposome band by in-gel fluorescence (Fig. 4 *B*) and a radioligand binding assay revealed that the receptor was reconstituted in a conformation that was both fluorescent and able to bind NT ($K_d = 0.6 \pm 0.2$ nM) (Fig. 2 *A*), with a recovered receptor yield of 49.6% ± 14.9% in the proteoliposome fraction (relative to the amount of fluorescent receptor added to the reconstitution). The in-gel fluorescence analysis (Fig. 4 *B*) did not reveal the presence of any free CFP or YFP in the reconstitution samples. Tryptic digestion of the reconstituted receptors and a subsequent densitometry analysis of cleavage fragments separated by SDS-PAGE and visualized by in-gel fluorescence suggested that 53% ± 2% ($n = 4$) of the reconstituted receptor was oriented with the ligand-binding site on the outer face of the proteoliposomes (data not shown). This suggests that the receptor is inserted into the liposomes in a random orientation, which was suggested to be a property of DDM-mediated reconstitutions of membrane proteins (39).

The FRET measurements were performed on reconstituted T43NTS1-eCFP/eYFP samples, both in the absence and presence of NT. The receptor density was controlled by varying the initial lipid/protein ratio of reconstitutions between 6000:1 and 1000:1 (eCFP/eYFP molar ratio of 1:1 ± 0.03). Significant FRET was observed in all samples (Fig. 5 and Table 1), and was independent of the presence of NT agonist. In addition, apparent FRET efficiency did not vary significantly with receptor density, suggesting that the FRET is caused by a true NTS1-NTS1 interaction in the membrane. If FRET arises from random collisions, a pseudolinear increase in FRET efficiency with receptor density would be expected, as was reported in BRET studies with other GPCRs (16,40).

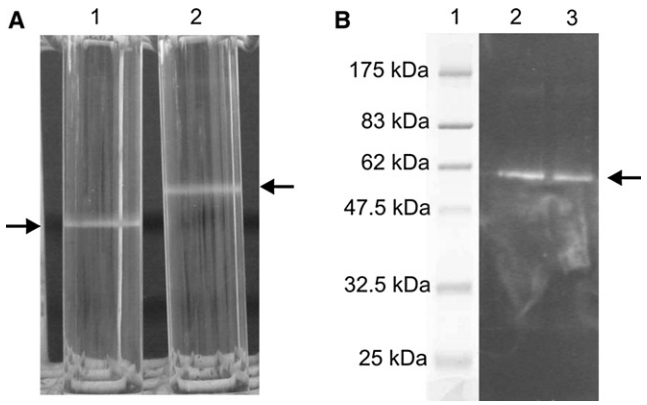

FIGURE 4 Reconstitution of fluorescence-tagged NTS1 into BPL vesicles. (*A*) Sucrose density gradient centrifugation of T43NTS1-eCFP/eYFP reconstitution samples. Initial lipid/protein ratios were 1000:1 (tube 1) and 2000:1 (tube 2). Proteoliposome bands are indicated by arrows. (*B*) In-gel fluorescence analysis of proteoliposome bands harvested from density gradients. Samples were separated by SDS-PAGE, using a 12% Tris-Glycine gel. Lane 1, molecular mass marker; lane 2, 1000:1; lane 3, 2000:1. Fluorescent receptor bands are indicated by arrow.

Competition experiments suggest a specific receptor-receptor interaction

The measurement of FRET efficiency was performed in reconstituted samples containing varying amounts of non-fluorescently tagged receptor. A constant initial molar ratio of lipid/fluorescent protein was used for each reconstitution (6000:1). Only the amount of untagged NTS1 receptor was varied, thereby maintaining, as far as possible, a constant density of fluorescent receptor in the membrane. The apparent FRET efficiency decreased linearly with an increasing molar percentage of untagged receptor (Fig. 6). This is indicative of a specific receptor-receptor interaction, rather than bystander FRET, and the linear relationship supports the suggestion of an NTS1 homodimer, because deviation from linearity would be expected for higher-order multimers or aggregates (41). In addition, this result rules out the possibility that the observed multimerization of fluorophore-tagged receptors is driven by interactions between eCFP/eYFP fluorescent proteins, which were previously shown to dimerize at high concentrations (42).

NTS1 forms a homodimer in reconstituted membranes

Further experiments, designed to elucidate the precise multimerization state of the receptor, were performed. The donor (eCFP)/acceptor (eYFP) ratio was varied by adding purified eCFP-tagged and eYFP-tagged receptor to the reconstitutions in the desired proportions. The ratio was confirmed using fluorescence intensity measurements of the donor and acceptor after reconstitution. Control of the donor/acceptor ratio is essential for a correct quantitative analysis of FRET efficiency. Care was taken to keep the overall fluorescent receptor density constant for each sample (initial lipid/protein molar ratio of 6000:1), thereby removing interpretation complications that could arise from potential bystander FRET, which would vary pseudolinearly with receptor density (16,43).

Apparent FRET efficiency decreased as the proportion of NTS1-eYFP, expressed as a percentage of total fluorescent receptor, increased (Fig. 7 *A*). This result is to be expected for a multimeric interaction, because an increased proportion of acceptor increases the likelihood that an acceptor monomer will be in a multimeric complex containing no donor fluorophores (and hence will not be amenable to FRET) (Fig. 7 *B*). Such a relationship should not be observed if FRET is caused

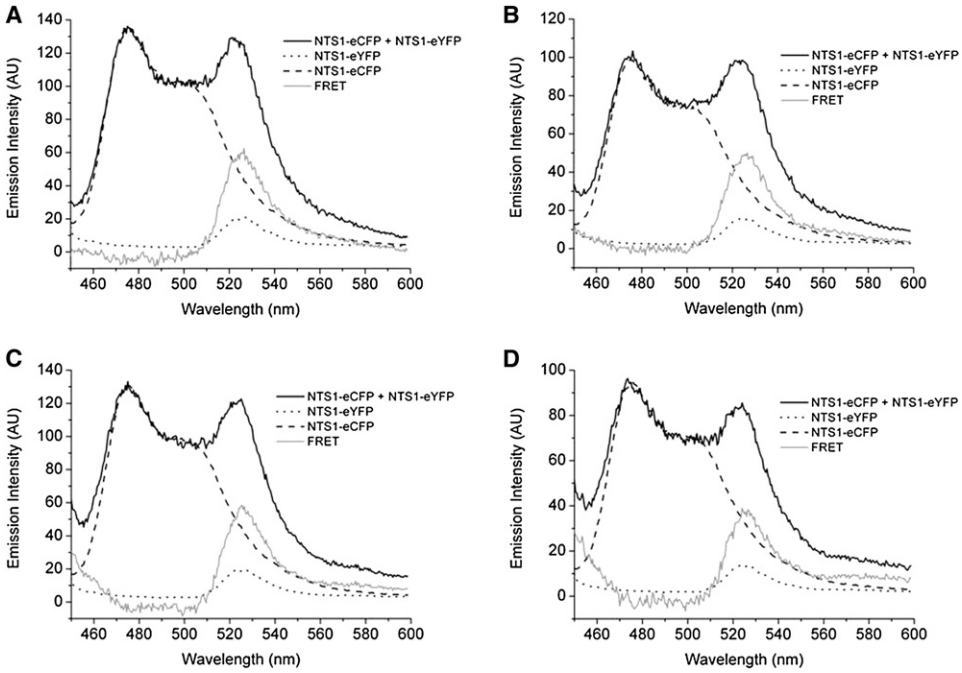

FIGURE 5 Use of FRET to detect multimerization of lipid-reconstituted T43NTS1-eCFP/eYFP at varied receptor densities. Reconstitution samples had starting lipid/protein ratios of 1000:1 (*A*), 2000:1 (*B*), 4000:1 (*C*), and 6000:1 (*D*). Samples were excited at λ_{max}^{CFP} (440 nm), and fluorescence emission was detected by scanning fluorometry. Fluorescence emission attributable to FRET (*gray solid line*) was determined by subtracting normalized emission spectrum of a T43NTS1-eCFP-only sample (*black dashed line*) and normalized emission spectrum of a T43NTS1-eYFP-only sample (*black dotted line*) from emission spectrum of the mixed T43NTS1-eCFP and T43NTS1-eYFP sample (*black solid line*).

by random collisions, provided that (as is the case here) the total receptor density is kept constant (16).

To distinguish between dimers and higher-order oligomers, the experimental results were compared with modeled FRET curves, derived using an equation that describes the probability of forming FRET-competent complexes as a function of the number of receptors within a complex (40,44,45). The experimental data fit closely to the model curve for the dimer (Fig. 7 *C*), suggesting that the average stoichiometry of NTS1 in the reconstituted membranes is a dimer. Assuming that the receptor exists in equilibrium between monomer and dimer, it is possible to estimate the proportion of receptor that exists in a multimeric versus monomeric conformation. The equation presented in the legend of Fig. 7 can be modified to account for a dimeric receptor with a proportion of monomeric population (Supporting Material). Fitting of the modified equation to the experimental data presented in Fig. 7 *A* suggests that 88.7% ± 0.2% of the reconstituted receptor molecules are in dimeric form at this receptor density.

TABLE 1 Apparent FRET efficiency of T43NTS1-eCFP/eYFP reconstituted samples in the presence and absence of 50 μM NT

	Apparent FRET efficiency (%)	
Initial lipid/protein ratio	No NT	NT (50 μM)
1000	10.4	10.3
2000	12.0	11.3
4000	11.4	11.5
6000	11.6	11.6
Mean (± error)	11.4 ± 0.3	11.2 ± 0.3

Apparent FRET efficiency was calculated from emission spectra: ((integrated FRET curve)/(integrated emission curve obtained on direct excitation of eYFP at λ_{max}^{YFP})) × 100.

DISCUSSION

This study demonstrates that FRET measurements can be applied successfully to the study of the multimerization state of GPCRs reconstituted into model lipid membrane systems. The FRET analysis of eCFP-tagged and eYFP-tagged receptors in detergent solution suggests that NTS1 is monomeric at receptor concentrations of up to 200 nM. This is in agreement with a previous study of NTS1, which suggested that although NTS1 can dimerize in detergent solution, such dimerization is inhibited by the relatively high concentrations of detergent used in the purification procedure (20). It is therefore possible that decreased detergent concentrations or increased receptor concentrations could drive the dimerization reaction in detergent solution.

In contrast, the results of FRET experiments with lipid-reconstituted NTS1 demonstrate constitutive NTS1 multimerization at receptor densities comparable to recent in vivo RET studies of GPCR multimerization (16,40). Rigorous control experiments involving the variation of receptor density, variation of donor/acceptor ratio, and competition with untagged receptor were reported as essential for the verification of the presence of true receptor multimers in RET studies (16). Here, in the first (to our knowledge) comprehensive application of these controls to a RET study of a GPCR in an in vitro system, we confirmed that FRET arose from a true receptor-receptor interaction between NTS1 monomers, rather than from random receptor collisions in the membrane or from multimerization mediated by dimerization of eCFP/eYFP

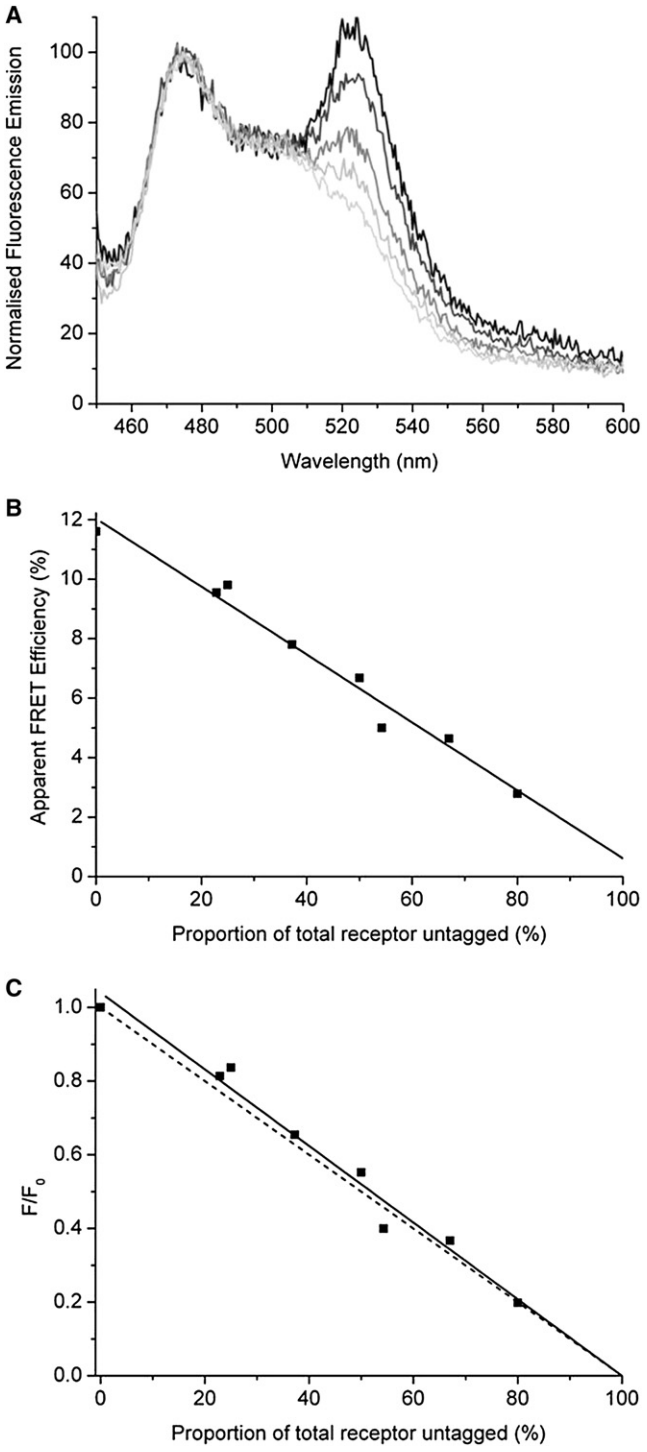

FIGURE 6 FRET analysis of lipid-reconstituted eCFP-tagged and eYFP-tagged NTS1 in the presence of untagged NTS1. (*A*) Samples were excited at λ_{max}^{CFP} (440 nm), and fluorescence emission was detected by scanning fluorometry. Samples contained 0%, 25%, 50%, 67%, and 80% untagged NTS1 (*dark to light traces*). The lipid/fluorescent receptor ratio for each reconstitution was kept constant. (*B*) Increasing molar percentage of untagged receptor caused a decrease in apparent FRET efficiency, which was fitted linearly (*black line*). From the fit, a sample containing 100% untagged receptor would yield a FRET efficiency of 0.6%. This represents the ''bystander FRET'' caused by random collisions at this density of fluorescent receptor. (*C*) Alternative representation of results. F, apparent FRET efficiency with bystander FRET subtracted. $F_o = F$ in the absence of competitor. Data were fitted linearly (*black line*). The theoretical competition curve for an NTS1 homodimer is also shown (*dotted line*). Deviation from linearity would be expected for higher-order multimers.

fluorescent proteins. A comparison with theoretical calculations showed that a homodimer model, rather than models for higher-order interactions or aggregation artifacts, best fits the experimental data. This result is in agreement with a previous suggestion that constitutive dimerization is a property shared by many (though not all) GPCRs of the Family A subtype (7–9).

The final lipid/protein molar ratios of proteoliposome samples were estimated from the isopyknic position on sucrose gradients (see the Supporting Material). The lipid/protein molar ratios were significantly lower than the starting ratios (between 576.4 ± 27.0 for the 1000:1 initial ratio, and 1033.3 ± 88.8 for the 6000:1 initial ratio). A similar result was evident for the detergent-mediated reconstitution of rhodopsin into asolectin liposomes, where an initial lipid/protein molar ratio of 10,000:1 resulted in a final ratio of 1000:1 after reconstitution (21). The authors attributed this phenomenon to the observation that 90% of the rhodopsin receptors inserted into only 10% of the available liposomes. In addition, Biobeads have been shown to adsorb small amounts of lipid during detergent removal (38), which could also be a contributory factor.

Despite the decrease in lipid/protein ratio during the reconstitution, the final receptor densities in the reconstituted samples were low, relative to previous RET studies of GPCRs. The receptor densities in T43NTS1-eCFP/eYFP reconstituted samples were calculated from the lipid/protein molar ratio to be between 0.13 (6000:1 initial) and 0.24 (1000:1 initial) receptors per 10,000 Å^2. In a previous in vivo study of the β-adrenergic-receptor GPCR fused with luciferase and green fluorescent protein (GFP) (40), constant BRET efficiency was observed at expression levels between 1.4–26 pmol/mg of membrane protein, indicating a true receptor-receptor interaction and low bystander BRET. An increase of the expression level to 47 pmol/mg (2.4 receptor molecules per 10,000 Å^2) and higher gave a large increase in BRET efficiency, attributed to bystander BRET. This receptor density is ~10-fold higher than calculated for the NTS1 reconstituted samples, suggesting that little contribution from bystander FRET should be expected in reconstituted samples, supporting the conclusion that a true multimeric receptor complex is forming.

The apparent efficiency of FRET at a donor/acceptor ratio of 1:1 (11.2% ± 0.3% and 11.4% ± 0.3% in the absence and presence of NT, respectively) compares favorably with the efficiency observed for FRET between eCFP-tagged and eYFP-tagged yeast α-factor receptor in vivo (11.5% ± 2.2%), a GPCR that is widely believed to dimerize

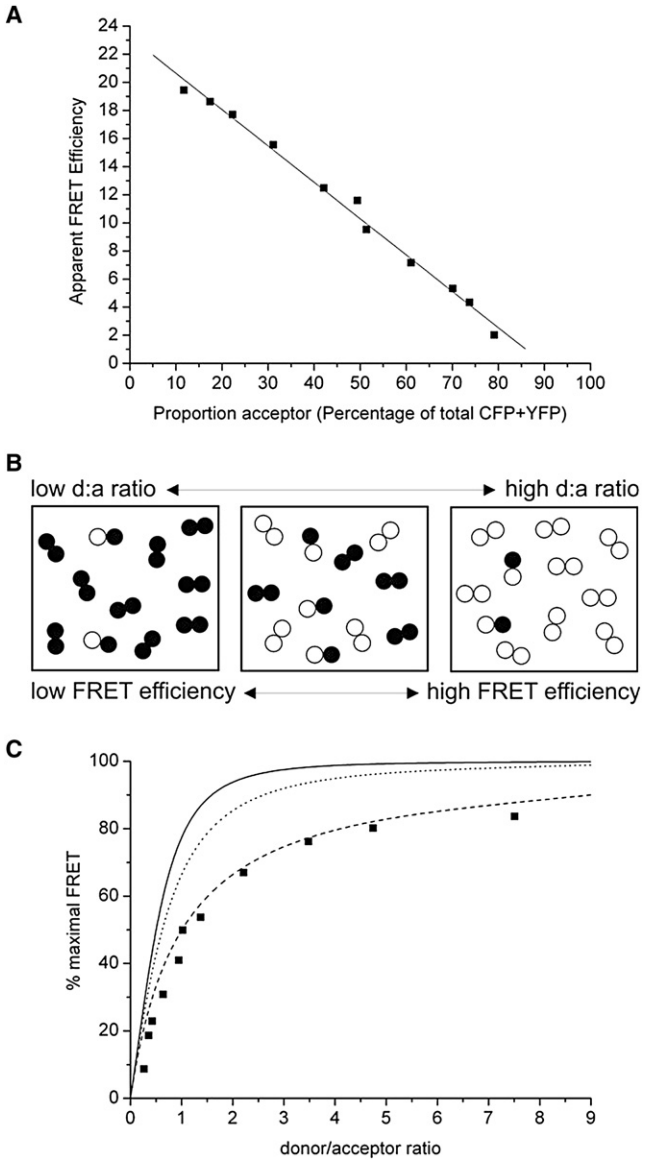

FIGURE 7 FRET analysis of NTS1-eCFP/eYFP reconstituted into BPL liposomes at varying donor/acceptor ratios. (*A*) Apparent FRET efficiency is plotted versus percentage of total receptor, which is acceptor-tagged. Overall receptor density was kept constant (6000:1 starting lipid/protein ratio, confirmed by identical densities on sucrose gradients). The *y* intercept gives a measure of F_{max}, the FRET that would be observed in the presence of a vast excess of donor fluorophore (23.2% ± 0.4%). (*B*) Schematic depiction of likelihood of tagged receptors forming FRET-competent complexes as donor/acceptor (d:a) ratio is varied (•, *acceptors*; ○, *donors*). (*C*) Comparison of experimental data (*solid squares*) with theoretical curves for the dimer (*dashed line*), trimer (*dotted line*), and tetramer (*solid line*). Theoretical curves are based on the probability that an eYFP-tagged receptor is in a complex with one or more eCFP-tagged receptors (and hence in a FRET-capable complex): $[(a+d)^n - a^n - d^n]/[(a+d)^n - a^n - d^n + na^n]$, where *n* is the number of receptor molecules in the complex, and *a* and *d* are relative concentrations of acceptor and donor, respectively (40,44,45).

constitutively (17). A comparable FRET efficiency was observed for eCFP-tagged and eYFP-tagged C5a receptor in vivo (12.6% ± 3.0%) (46). To calculate the precise efficiency of FRET, which in turn allows the quantification of interfluorophore distance, a "corrected FRET efficiency" term can be calculated. This is a modification of the apparent FRET efficiency, to take into account the different extinction coefficients of the donor and acceptor fluorophores at their respective λ_{max} excitations (Eq. 4). In the presence of a vast excess of donor fluorophore, the apparent FRET efficiency (F_{max}) was determined to be 23.2% ± 0.4% (Fig. 7 *A*). This corresponds to a corrected FRET efficiency of 59.1% ± 1.0%, and an average interfluorophore distance of 42.9 ± 0.8 Å. This distance is similar to that derived from recent atomic-force microscopy studies on rhodopsin from mouse rod outer segments, which showed rhodopsin organized within paracrystalline arrays with densely packed, double rows of receptor (47). Models of atomic-force microscopy images revealed contact dimers with an intradimeric monomer-monomer distance of 38 Å, and a distance of 46 Å between the nearest neighbors from different double rows (47–49).

The role of a constitutive GPCR dimer as the functional signaling unit is yet to be demonstrated conclusively, although it is thought to have important functional implications, including cell-surface expression, ligand binding, signaling, and receptor trafficking (8). The saturation binding data for NTS1 in detergent solution and in lipid bilayers revealed no evidence of cooperative binding (Fig. 2 *B*) or any difference in binding affinity for the NT-NTS1 interaction. Therefore, it appears that dimerization does not serve to modulate the mechanism of NT binding, at least in the absence of other cellular components. This result is in agreement with previous binding data for the NT-NTS1 interaction in the membrane environment, including synaptic membranes (34) and cell lines (6,35) that did not reveal any cooperativity. However, our result is in contradiction with a previous study of NTS1 in detergent solution (20), which suggested that cooperative binding was driven by the monomer-dimer transition. In addition, the minimal unit for GPCR function is still debated. In the case of rhodopsin, the existence of dimers in vivo is still questioned (50), with separate studies supporting either one (49) or two (51) G-protein heterotrimers per receptor dimer. The demonstration that single β-adrenergic-receptor monomers, reconstituted into high-density lipoprotein phospholipid bilayer particles, can efficiently activate heterotrimeric G-proteins suggests that the GPCR monomer is the minimal functional unit necessary for signaling in this case (52). In contrast, the leukotriene B_4 receptor, another GPCR of the family A subtype that dimerizes and forms a heteropentameric complex with a single G-protein heterotrimer (11), was shown to demonstrate full G-protein activation when only a single subunit of the dimer was occupied with an agonist (53).

The reconstitution of purified T43NTS1-eCFP/eYFP into BPL vesicles appears to provide a useful minimal, in vitro experimental system for the study of NTS1 multimerization. Increasing the complexity of the system through the addition

of other signaling components could be envisaged in a quantitative, controlled manner. In addition, our results demonstrate the potential of the system in the study of the dimerization interface, the location and specificity of which are still controversial topics in the GPCR field (8). The importance of specific lipids is also emphasized, both in the maintenance of a ligand-binding conformation of NTS1 and in multimerization interactions. This approach could provide useful insights into the multimerization states of other GPCRs for which expression and purification protocols can be established.

SUPPORTING MATERIAL

Additional materials, methods, calculations, and references are available at http://www.biophysj.org/biophysj/supplemental/S0006-3495(08)00081-7.

We thank Dr. Achilles Kapanidis and Dr. Michael Heilemann (Oxford University Physics) for their advice on FRET analysis, Dr. Reinhard Grisshammer for the donation of his NTS1B construct, Dr. Huanting Liu and Professor Jim Naismith at the University of St. Andrews for the donation of the TeV-His_6 construct, and Prof. Stuart Ferguson for the use of his Gel Doc machine.

We acknowledge the Medical Research Council, the Biotechnology and Biological Sciences Research Council, and the United Kingdom Bionanotechnology Interdisciplinary Research Collaboration for funding this work.

REFERENCES

1. Vassilatis, D. K., J. G. Hohmann, H. Zeng, F. Li, J. E. Ranchalis, et al. 2003. The G protein-coupled receptor repertoires of human and mouse. *Proc. Natl. Acad. Sci. USA.* 100:4903–4908.
2. Ji, T. H., and I. Ji. 1998. G protein-coupled receptors. *J. Biol. Chem.* 28:17299–17302.
3. Iyengar R., J. D. Hildebrandt, editors. 2002. G Protein-coupled pathways. Parts A, B & C. Methods in Enzymes, Vols. 343–345.
4. Vanti, W. B., S. Swaminathan, R. Blevins, J. A. Bonini, B. F. O'Dowd, et al. 2001. Patent status of the therapeutically important G-protein-coupled receptors. *Expert Opin. Ther. Pat.* 11:1861–1887.
5. Carraway, R. E., and S. E. Leeman. 1973. Discovery of neurotensin. *J. Biol. Chem.* 248:6845–6861.
6. Tanaka, K., M. Masu, and S. Nakanishi. 1990. Structure and functional expression of the cloned rat neurotensin receptor. *Neuron.* 4:847–854.
7. Lee, S. P., B. F. O'Dowd, and S. R. George. 2003. Homo- and hetero-oligomerization of G protein-coupled receptors. *Life Sci.* 74:173–180.
8. Milligan, G. 1768. 2007. G protein-coupled receptor dimerisation: molecular basis and relevance to function. Biochim. Biophys. Acta. 4:825–835.
9. Milligan, G., and M. Bouvier. 2005. Methods to monitor the quaternary structure of G protein-coupled receptors. *FEBS J.* 272:2914–2925.
10. Milligan, G. 2004. G protein-coupled receptor dimerization: function and ligand pharmacology. *Mol. Pharmacol.* 66:1–7.
11. Baneres, J. L., and J. Parello. 2003. Structure-based analysis of GPCR function: evidence for a novel pentameric assembly between the dimeric leukotriene B4 receptor BLT1 and the G-protein. *J. Mol. Biol.* 329:815–829.
12. Cvejic, S., and L. A. Devi. 1997. Dimerization of the delta opioid receptor: implication for a role in receptor internalization. *J. Biol. Chem.* 272:26959–26964.
13. Hebert, T. E., S. Moffett, J. P. Morello, T. P. Loisel, D. G. Bichet, et al. 1996. A peptide derived from a beta2-adrenergic receptor transmembrane domain inhibits both receptor dimerization and activation. *J. Biol. Chem.* 271:16384–16392.
14. Monnot, C., C. Bihoreau, S. Conchon, K. M. Curnow, P. Corvol, et al. 1996. Polar residues in the transmembrane domains of the type 1 angiotensin II receptor are required for binding and coupling. Reconstitution of the binding site by co-expression of two deficient mutants. *J. Biol. Chem.* 271:1507–1513.
15. Lee, C., I. Ji, K. Ryu, Y. Song, P. M. Conn, et al. 2002. Two defective heterozygous luteinizing hormone receptors can rescue hormone action. *J. Biol. Chem.* 277:15795–15800.
16. James, J. R., M. I. Oliveira, A. M. Carmo, A. Iaboni, and S. J. Davis. 2006. A rigorous experimental framework for detecting protein oligomerization using bioluminescence resonance energy transfer. *Nat. Methods.* 3:1001–1006.
17. Overton, M. C., and K. J. Blumer. 2002. Use of fluorescence resonance energy transfer to analyze oligomerization of G-protein-coupled receptors expressed in yeast. *Methods.* 27:324–332.
18. Perron, A., N. Sharif, P. Sarret, T. Stroh, and A. Beaudet. 2006. NTS2 modulates the intracellular distribution and trafficking of NTS1 via heterodimerization. *Biochem. Biophys. Res. Commun.* 353:582–590.
19. Martin, S., V. Navarro, J. P. Vincent, and J. Mazella. 2002. Neurotensin receptor-1 and -3 complex modulates the cellular signaling of neurotensin in the HT29 cell line. *Gastroenterology.* 123:1135–1143.
20. White, J. F., J. Grodnitzky, J. M. Louis, L. B. Trinh, J. Shiloach, et al. 2007. Dimerization of the class A G protein-coupled neurotensin receptor NTS1 alters G protein interaction. *Proc. Natl. Acad. Sci. USA.* 104:12199–12204.
21. Mansoor, S. E., K. Palczewski, and D. L. Farrens. 2006. Rhodopsin self-associates in asolectin liposomes. *Proc. Natl. Acad. Sci. USA.* 103:3060–3065.
22. White, J. F., T. B. Loc, J. Shiloach, and R. Grisshammer. 2004. Automated large-scale purification of a G protein-coupled receptor for neurotensin. *FEBS Lett.* 564:289–293.
23. Luca, S., J. F. White, A. K. Sohal, D. V. Filippov, J. H. van Boom, et al. 2003. The conformation of neurotensin bound to its G protein-coupled receptor. *Proc. Natl. Acad. Sci. USA.* 100:10706–10711.
24. Harding, P. J., H. Attrill, S. Ross, J. R. Koeppe, A. N. Kapanidis, et al. 2007. Neurotensin receptor type 1: *Escherichia coli* expression, purification, characterization and biophysical study. *Biochem. Soc. Trans.* 35:760–763.
25. Cubitt, A. B., L. A. Woollenweber, and R. Heim. 1999. Understanding structure-function relationships in the *Aequorea victoria* green fluorescent protein. *Methods Cell Biol.* 58:19–30.
26. Rizzo, M. A., G. H. Springer, B. Granada, and D. W. Piston. 2004. An improved cyan fluorescent protein variant useful for FRET. *Nat. Biotechnol.* 22:445–449.
27. Patterson, G., R. N. Day, and D. Piston. 2001. Fluorescent protein spectra. *J. Cell Sci.* 114:837–838.
28. Tsien, R. Y. 1998. The green fluorescent protein. *Annu. Rev. Biochem.* 67:509–544.
29. Clegg, R. M. 1992. Fluorescence resonance energy transfer and nucleic acids. *Methods Enzymol.* 211:353–388.
30. Mukhopadhyay, J., A. N. Kapanidis, V. Mekler, E. Kortkhonjia, Y. W. Ebright, et al. 2001. Translocation of sigma(70) with RNA polymerase during transcription: fluorescence resonance energy transfer assay for movement relative to DNA. *Cell.* 106:453–463.
31. Drew, D., G. von Heijne, P. Nordlund, and J. W. de Gier. 2001. Green fluorescent protein as an indicator to monitor membrane protein overexpression in Escherichia coli. *FEBS Lett.* 507:220–224.
32. Drew, D., M. Lerch, E. Kunji, D. Slotboom, and J. W. de Gier. 2006. Optimisation of membrane protein overexpression and purification using GFP fusions. *Nat. Methods.* 3:303–313.
33. Tucker, J., and R. Grisshammer. 1996. Purification of a rat neurotensin receptor expressed in *Escherichia coli*. *Biochem. J.* 317:891–899.
34. Kitagbi, P., R. E. Carraway, J. V. Rietschoten, C. Granier, J. L. Morgat, et al. 1977. Neurotensin: specific binding to synaptic membranes from rat brain. *Proc. Natl. Acad. Sci. USA.* 74:1846–1850.

35. Vita, N., P. Laurent, S. Lefort, P. Chalon, X. Dumont, et al. 1993. Cloning and expression of a complementary DNA encoding a high affinity human neurotensin receptor. *FEBS Lett.* 317:139–142.

36. Rigaud, J. L., M. T. Paternostre, and A. Bluzat. 1988. Mechanisms of membrane protein insertion into liposomes during reconstitution procedures involving the use of detergents. 2. Incorporation of the light-driven proton pump bacteriorhodopsin. *Biochemistry.* 27:2677–2688.

37. Lambert, O., D. Levy, J. L. Ranck, G. Leblanc, and J. L. Rigaud. 1998. A new ''gel-like'' phase in dodecyl maltoside-lipid mixtures: implications in solubilisation and reconstitution studies. *Biophys. J.* 74: 918–930.

38. Rigaud, J. L., G. Mosser, J. J. Lacapere, A. Olofsson, D. Levy, et al. 1997. Bio-Beads: an efficient strategy for two-dimensional crystallisation of membrane proteins. *J. Struct. Biol.* 118:226–235.

39. Knol, J., K. Sjollema, and B. Poolman. 1998. Detergent-mediated reconstitution of membrane proteins. *Biochemistry.* 37:16410–16415.

40. Mercier, J. F., A. Salahpour, S. Angers, A. Breit, and M. Bouvier. 2002. Quantitative assessment of beta 1- and beta 2-adrenergic receptor homo- and heterodimerization by bioluminescence resonance energy transfer. *J. Biol. Chem.* 277:44925–44931.

41. Ayoub, M. A., C. Couturier, E. Lucas-Meunier, S. Angers, P. Fossier, et al. 2002. Monitoring of ligand-independent dimerization and ligand-induced conformational changes of melatonin receptors in living cells by bioluminescence resonance energy transfer. *J. Biol. Chem.* 277:21522–21528.

42. Phillips, G. N., Jr. 1997. Structure and dynamics of green fluorescent protein. *Curr. Opin. Struct. Biol.* 7:821–827.

43. Kenworthy, A. K., and M. Edidin. 1998. Distribution of a glycosylphosphatidylinositol-anchored protein at the apical surface of MDCK cells examined at a resolution of <100 Å using imaging fluorescence resonance energy transfer. *J. Cell Biol.* 142:69–84.

44. Veatch, W., and L. Stryer. 1977. The dimeric nature of the gramicidin A transmembrane channel: conductance and fluorescence energy transfer studies of hybrid channels. *J. Mol. Biol.* 113:89–102.

45. Li, M., L. G. Reddy, R. Bennett, N. D. Silva, Jr., L. R. Jones, et al. 1999. A fluorescence energy transfer method for analyzing protein oligomeric structure: application to phospholamban. *Biophys. J.* 76:2587–2599.

46. Floyd, D. H., A. Geva, S. P. Bruinsma, M. C. Overton, K. J. Blumer, et al. 2003. C5a receptor oligomerization. II. Fluorescence resonance energy transfer studies of a human G protein-coupled receptor expressed in yeast. *J. Biol. Chem.* 278:35354–35361.

47. Liang, Y., D. Fotiadis, S. Filipek, D. A. Saperstein, K. Palczewski, et al. 2003. Organization of the G protein-coupled receptors rhodopsin and opsin in native membranes. *J. Biol. Chem.* 278:21655–21662.

48. Fotiadis, D., B. Jastrzebska, A. Philippsen, D. J. Muller, K. Palczewski, et al. 2006. Structure of the rhodopsin dimer: a working model for G-protein-coupled receptors. *Curr. Opin. Struct. Biol.* 16:252–259.

49. Fotiadis, D., Y. Liang, S. Filipek, D. A. Saperstein, A. Engel, et al. 2004. The G protein-coupled receptor rhodopsin in the native membrane. *FEBS Lett.* 564:281–288.

50. Chabre, M., and M. le Maire. 2005. Monomeric G-protein-coupled receptor as a functional unit. *Biochemistry.* 44:9395–9403.

51. Dell'Orco, D., M. Seeber, and F. Fanelli. 2007. Monomeric dark rhodopsin holds the molecular determinants for transducin recognition: insights from computational analysis. *FEBS Lett.* 581:944–948.

52. Whorton, M. R., M. P. Bokoch, S. G. Rasmussen, B. Huang, R. N. Zare, et al. 2007. A monomeric G protein-coupled receptor isolated in a high-density lipoprotein particle efficiently activates its G protein. *Proc. Natl. Acad. Sci. USA.* 104:7682–7687.

53. Damian, M., A. Martin, D. Mesnier, J. P. Pin, and J. L. Baneres. 2006. Asymmetric conformational changes in a GPCR dimer controlled by G-proteins. *EMBO J.* 25:5693–5702.